Proceedings World Geothermal Congress 2015
Melbourne, Australia, 19-25 April 2015

Scouting for Permeable Structures in Geothermal Systems Using Soil Gas Radon

Jigo W. Mismanos and Atoz A. Vasquez

Energy Development Corporation, 38/F One Corporate Centre, Pasig City, Philippines 1605

mismanos.jw@energy.com.ph

Keywords: radon, soil gas, permeability, Leyte, Mahanagdong

ABSTRACT

Radon (^{222}Rn) is a radioactive gas with a half-life of 3.8 days, produced by the decay of ^{238}U. Anomalous accumulation of radon in soil gas can be indicative of rapid vertical transport through permeable structures that serve as pathways for deep-sourced radon. For this property, radon has been elaborately investigated in several volcanic, seismic, and geothermal studies. The application of soil radon gas mapping to permeability prospecting was tested in areas of known permeability characteristics at the Leyte Geothermal Production Field, Philippines. Using alpha spectroscopic radon detectors, 150m-spaced gridded measurements were conducted in Mahanagdong Sector, LGPF. In general, the mapped high soil radon anomalies are situated at structural intersections and segments that were reported by drilling to exhibit good permeability characteristics. Low radon concentrations were likewise observed over structures known to have poor permeability.

1. INTRODUCTION

Radon (^{222}Rn) is a naturally-occurring, colorless, odorless, radioactive gas belonging to the ^{238}U decay chain. It is the most abundant radon isotope and it has a half-life of only 3.8 days. Its intermediate parent is radium (^{226}Ra) and it undergoes alpha decay to become ^{218}Po.

Upon decay of radium, radon escapes from the mineral grains by radioactive recoil, *i.e.*, the opposite force created by the alpha particle to conserve momentum upon decay (Satomi and Kruger, 1982). Most of the kinetic energy is carried by the alpha particle and only a fraction is carried by the resulting radon atom (Tanner, 1964). The energy at recoil may be sufficient to carry it from the mineral to its surroundings (Satomi and Kruger, 1982). Radon in the subsurface can migrate by diffusion and convection (Cox, 1980). The controls in these processes govern the distance that radon atoms can travel before undergoing significant radioactive decay. Diffusion is the main mechanism of radon release from the mineral grains, but is greatly limited by the short half-life of radon, especially if the pore spaces are saturated with water. In contrast, convection can extract radon gas of deeper origins through a rising gas/water column. In convection, the movement of subsurface fluids is the main transport mechanism of the radon atoms. Because of the faster velocity of transport, more radon is carried and there is less time for decay; hence, radon concentrations may become enriched in soil (Voltattorni and Lombardi, 2010). An established convective system must be in place to allow radon to migrate significant distances. The convection of radon can be lateral and vertical, the former being gravitational groundwater flow, while the latter pertaining to the movement of ground gas (Cox, 1980). The distance travelled by radon with groundwater is generally limited. Conversely, the vertical component or the movement of radon with upward-migrating gas is influenced by the ground permeability and temperature (*i.e.* heat driving the fluid convection). Distances of several hundred meters were calculated under suitable conditions of permeability and normal thermal gradients, and so greater transport distances can be expected in areas of elevated thermal gradients and better permeability (Cox, 1980).

Radon gas has been recognized as an important natural tracer in geologic systems because of 1) the ubiquity of its parent nuclides, 2) its enhanced mobility as a gas, 3) its inert chemical nature, 4) its short half-life, and 5) the ease of detection. Studies investigating spatial variations in soil radon showed that the presence of radon in large concentrations can be indicative of zones of brittle deformation with enhanced permeability (Voltattorni and Lombardi, 2010). Some studies also tried to correlate the sudden spikes in radon concentration with massive earthquake events (Richon *et al.*, 2003; Walia *et al.*, 2005). In geothermal exploration, most studies on radon are devoted to the search for structures and/or areas of high heat flow. The trends formed by high radon concentrations are usually considered as reflections of the trace of structures. In some cases, diffuse anomalies along a structure can also manifest due to fracture zones that may facilitate diffuse degassing (Voltattorni *et al.*, 2010).

In this study, the use of radon gas in confirming and predicting subsurface permeability in a geothermal reservoir is explored. The soil radon gas survey was conducted in the Mahanagdong Geothermal Field to compare soil radon signatures with actual permeability reported from wells. This can establish the basis for the surface exploration of permeable structures as good drilling targets.

2. GEOLOGIC SETTING

The Leyte Geothermal Field is situated in Leyte Island, where the Philippine Sea Plate subducts under the Philippine Mobile Belt (Figure 1). The geothermal system is hosted by andesitic volcano-sedimentary units intruded by microdioritic dikes. Numerous splays of the Philippine Fault cut across the geothermal system, providing permeability and fluid flow channels. The Mahanagdong Sector is located 5 km southeast of the contiguous Mahiao-Sambaloran-Malitbog system, separated by a cold impermeable block.

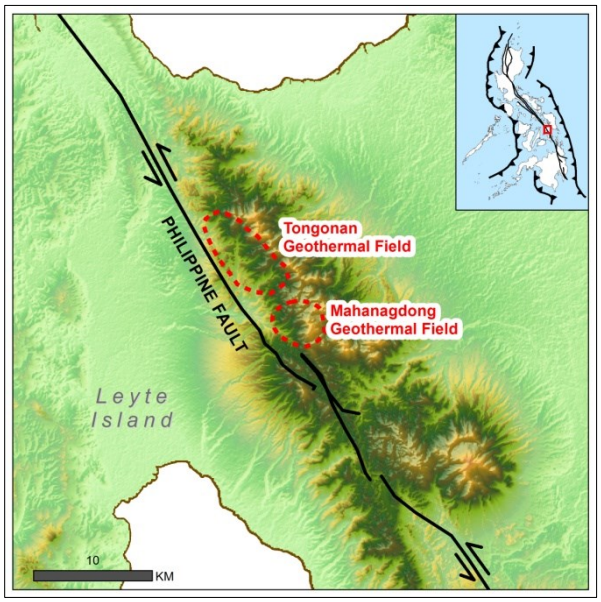

Figure 1: Geologic setting of the Leyte Geothermal Field in Leyte Island, Philippines

3. METHODS

A soil radon measurement survey was conducted in two areas in Mahanagdong Geothermal Field. The two sites cover an area where production and reinjection wells were directionally drilled. The production sector includes wells from Pad MG-5, while the reinjection sector encompasses all the wells at pad MG-RD1 (Figure 2). The measurement stations, roughly spaced at 150 m, were situated at fault traces and at fault blocks to have representative radon signatures in such settings. The survey covered a combined total area of 1.9 km^2.

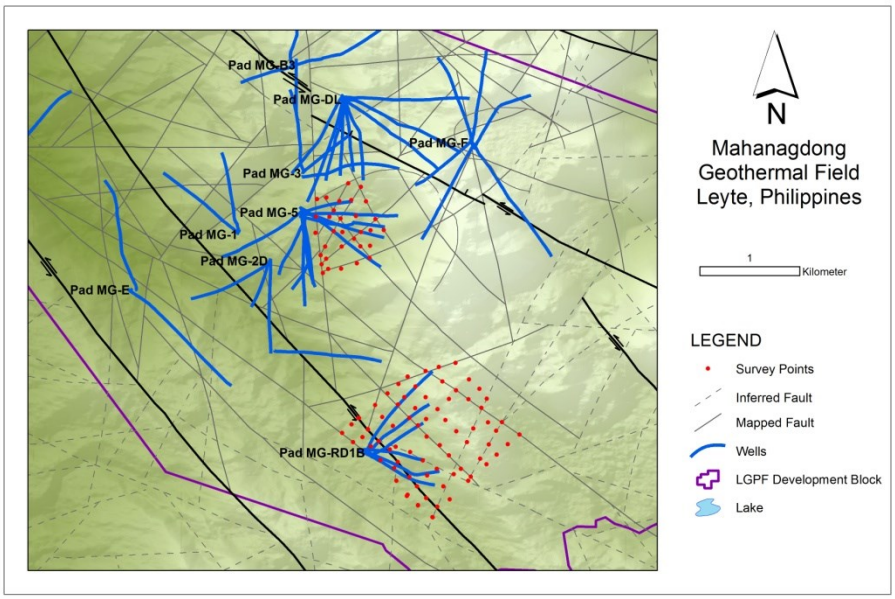

Figure 2: Map showing soil radon measurement grids in the Mahanagdong Geothermal Field

Soil radon concentrations were measured using a soil gas probe (SGP) and analogue radon sensor (ARS) (Figure 3) manufactured by SARAD GmBH. These instruments measure radon through alpha emission spectroscopy of decayed radon daughters. The SGP was placed inside a PVC pipe and buried in a vertical hole dug 1 m deep. This was connected to the ARS, which was hooked up to a 12-V power supply and a laptop PC (Figure 3). For each station, measurements were taken every minute over a 1.5-hour period.

The establishment of threshold values that would determine anomalous soil radon concentrations followed the method of Sinclair (1974). This method discriminates a data set into several population groups by looking at inflection points in a probability diagram. Contour maps of soil radon concentration were then produced. The distribution of high and anomalous radon concentrations was correlated with the traces of structures. The radon signatures were also compared with permeability characteristics as deduced from petrology, well geology, and drilling reports.

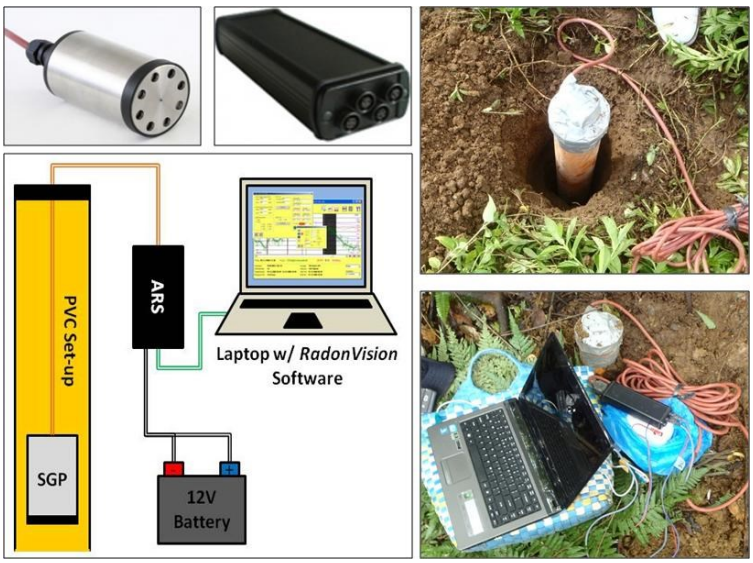

Figure 3: Clockwise from top left: soil gas probe, analogue radon sensor, picture of borehole and actual measurement set-up, and schematic diagram of instrument set-up

4. RESULTS AND DISCUSSIONS

A total of 73 and 32 stations were measured and occupied during the soil radon gas survey in MGRD1 and MG5, respectively. The concentration data sets followed a log-normal distribution. Log-normal transformation was applied to assume a normal distribution and perform population partitioning. The results of the population partitioning are summarized in Table 1.

Population	Proportion	No. of points	Range (Bq/m^3)	Type
MG-5 (PRODUCTION)				
A	12.50%	4	≥3098	Anomaly
B	87.50%	28	<3098	Background
MG-RD1 (REINJECTION)				
A	8.22%	6	≥8224	Anomaly
B	90.41%	65	284-8224	Background
C	1.37%	2	<284	Background

Table 1: Parameters of partitioned populations for surveyed areas in Mahanagdong

For MG-5, the anomaly was defined to be greater than 3098 Bq/m^3, comprising of four points. In MG-RD1, six points were identified to be anomalous, or greater than 8224 Bq/m^3. Color-contoured soil radon concentration maps were produced for MG-RD1 and MG-5. This aided in evaluating the empirical relationship between radon concentration and permeability. The anomalous radon concentrations identified in the above table were enclosed in black contours. Assessment of structural permeability was based on combined qualitative observations from drilling (faster rates of penetration, total or partial loss of circulation), geology and petrology (shearing, veins, vuggy texture, alteration minerals), and well completion test survey (waterloss surveys). The correlation of subsurface permeability and radon concentration is discussed in the succeeding sections.

4.1 Soil Radon in a "Production Sector" (MG-5)

In MG-5, the anomalously high radon concentrations were observed only in the northern portion of the map (in the area marked 1 and 2), which are centered at fault intersections (Figure 4). The North Mamban Fault was encountered by MG-5 wells targeted to the east. MG-36D and MG-27D indicated good permeability characteristics (shearing/veining, mud circulation losses, faster rates of penetration) in its intersection to this fault, while MG-5D, MG-18D, and MG-34D reported tight or poor permeability with this structure.

Although their values are below the indicated anomaly threshold, patches of slightly higher concentrations have been observed at some faults/fault intersections in Area 3 (Mantugop-B and North Mamban Faults), Area 4 (Mantugop-B & Lumpag Faults), and Area 5 (Mantugop-A & Lumpag Faults). The elevated radon in Anomaly 3 could be related with the permeable intersections of wells MG-33D and MG-39D with North Mamban Fault .Well MG-18D has one permeable zone with Mantugop-B, which could relate to the increased radon in Area 3. Similarly, MG-32D reported of a permeable zone in its intersection with Mantugop-B and Mantugop-A, which could explain the slightly higher concentration patches around Area 3 and 4. The elevated radon in 5 could be related with the close intersections of the parallel Mantugop Faults with the North Mamban Fault. For individual fault traces, the measured radon concentrations correlate only fairly with permeability. Wells that intersected segments of the Mantugop Faults (B, C, D), Lumpag Fault and North Mamban Fault, had differing reports of encountered permeability for each structure.

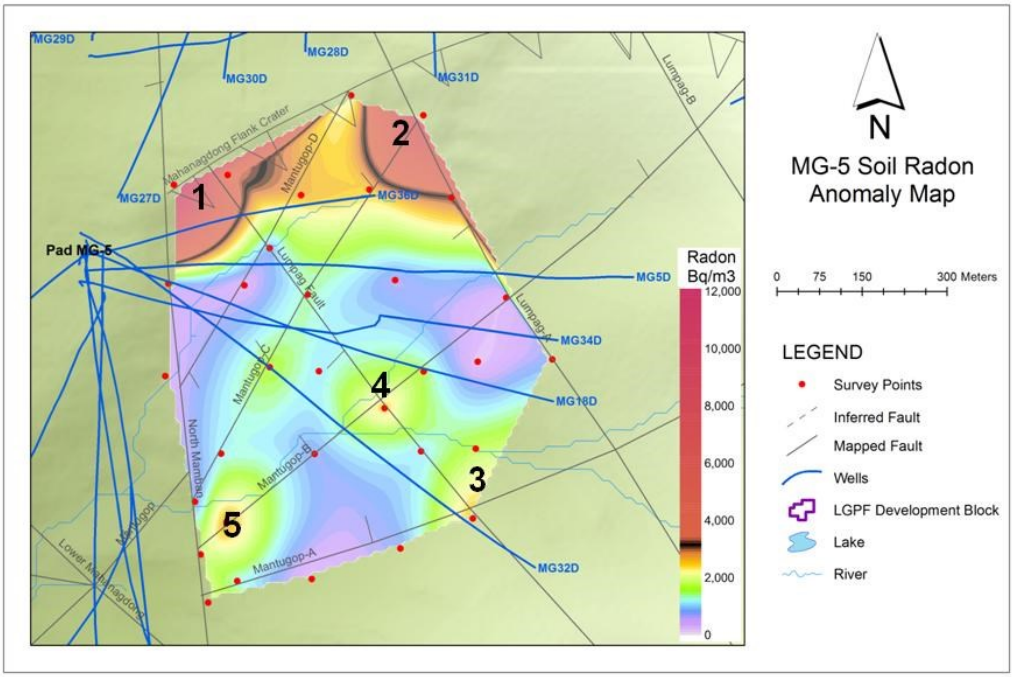

Figure 4: Soil radon anomaly map of MG-5 area

4.2 Soil Radon in a "Reinjection Sector" (MG-RD1)

The MG-RD1 anomaly map is presented in Figure 5. The anomalously high soil radon concentrations were observed in the western half of the surveyed area, which all lie at or near a fault trace. The highest radon concentration was recorded in the vicinity of Anomaly 1, which can be credited to the trace of the Macape Splay Fault. This could be an indication of the major permeable zone of MG-5RD associated with the overlap of Macape Splay and Lower Mahanagdong Fault.

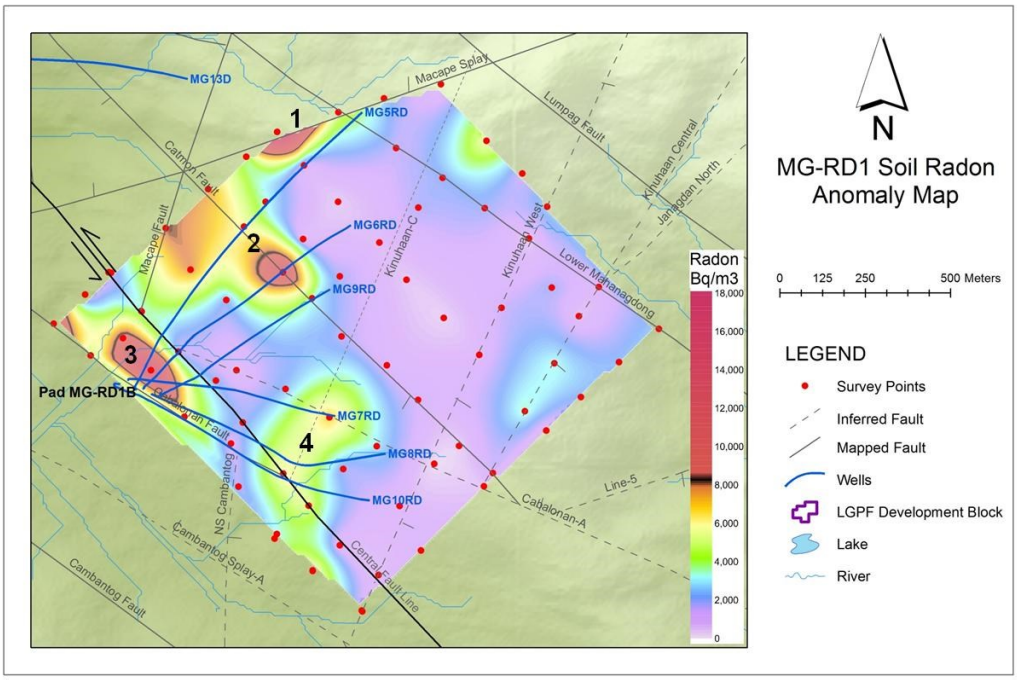

Figure 5: Soil radon anomaly map of MG-RD1 area

In Anomaly 2, the high soil radon measured in the upper segments of Catmon Fault corresponds to the good permeability reported at wells MG-5RD, MG-6RD and MG-9RD. However, the lower segment of Catmon Fault did not show the same high concentrations. Diffuse degassing of the Catmon and Macape Fault may have facilitated dispersion of this anomaly to the northeast between these structures. The high radon concentrations registered between the Cabalonan Fault and Central Fault Line are designated in Anomaly 3. Most survey points sited between these adjoining structures exhibited very high radon concentrations. This could perhaps be explained by good fracturing between the two structures, although since the anomaly is situated at the well

pads, vertical degassing pathways created by well-drilling or fracturing by reinjection could be probable reasons too. The high values of Anomaly 3 can be separated from Anomaly 2 by low values along most of the Central Fault Line (CFL). All the MG-RD1 wells intercepted the CFL and reported tight or poor permeability, indicated by weak shearing and minimal circulation losses.

Area No. 4 is the observed patch of high soil radon in the central south. The high radon in Cabalonan-A Fault agrees with good permeability indicators noted during intercept of MG-7RD and MG-8RD in this structure. The high concentration values might also correspond to permeability in Kinuhaan-C Fault, one of the markedly permeable structures intersected by MG-10RD. The trace of Kinuhaan-C could fairly approximate the alignment of high concentrations in this anomaly. Although the trace is only projected until it adjoins the Central Fault Line, it might probably even extend a little further southwest.

The eastern portion of the map, which is less dense with structures, is generally low in radon. The NE-SW trending (Kinuhaan West and Kinuhaan Central) and NW-SE trending faults (Catmon and Lower Mahanagdong) did not manifest any remarkably high radon concentrations. A group of low radon values is observed within the block bounded by the Catmon, Lower Mahanagdong and Kinuhaan West Faults. Low radon concentrations may be expected for the fault block lacking structural pathways for gas.

4.3 Difference of soil radon concentrations between MG-5 and MG-RD1

In general, most of the high radon anomalies were detected in faults and fault intersections. Also, the identified radon anomaly threshold is smaller in MG-5 compared to that of RD-1, indicating less intensity of degassing in the MG-5 area. This is perceived as the effect of the difference in reservoir pressure between the sectors, which has an effect on radon liberation from rocks. The emanating power of radon from reservoir rock is expected to be dependent on the following parameters: (1) rock type, (2) rock size distribution, (3) pore fluid density, (4) reservoir temperature, and (5) reservoir pressure (Kruger, et al. 1979). Among these factors, reservoir pressure is thought as the most significant between the two sectors. Kruger and others (1979) noted that radon emanation was increased when fractures in the formation remained open under applied pressure, then dropped to reference levels when the applied pressure was relieved. The applied pressure had a dilatational effect on the fractures, hence enhancing the release of radon from rocks to the reservoir. In that case, the difference in the observed values for MG-5 and MG-RD1 could be an effect of the difference in reservoir pressures between MG-5, where pressure drawdown is experienced, and MG-RD1, where pressure support is present because of injection.

5. CONCLUSIONS

The collected soil radon gas survey data follows log-normal distribution. From population partitioning, the anomalous soil radon concentrations were identified to be $\geq$8224 Bq/m^3 and $\geq$3098 Bq/m^3 for MG-RD1 and MG-5, respectively. Since the anomalies were derived using statistical methods, the differing threshold values arise from the distinct characteristics of data collected for each area. Most of the high radon anomalies were detected at faults/fault intersections. In general, the correlation of prominent high anomalies with good permeability reported by wells affirms the groundwork of this method. Caution in interpretations must still be effected as soil radon is sensitive to a number of factors, most of which are still under experimental observation.

Integration of this data with structural analysis and geophysical data, is anticipated to enhance pre-drilling knowledge on structural permeability. It is hoped that a good evaluation of this technique will be achieved after surveys and confirmation by drilling in other geothermal sites in the Philippines. This may be established as a reliable permeability exploration method for EDC's operating geothermal fields and exploration areas.

REFERENCES

Cox, M.E. Ground Radon Surveys for Geothermal Exploration in Hawaii. M.S. Thesis. University of Hawaii. U.S.A. (1980).

Kruger, P., Macias-C., L., Semprini, L. Radon Transect and Emanation Studies. Stanford Geothermal Workshop. Stanford, CA. (1979).

Richon, P. 1., Sabroux, J. C., Halbwachs, M., Vandemeulebrouck, J., Poussielgue, N., Tabbagh, J., & Punongbayan, R. Radon anomaly in the soil of Taal volcano, the Philippines: a likely precursor of the M 7.1 Mindoro earthquake (1994). *Geophysical Research Letters* (2003), 30(9).

Sinclair, A.J., Selection of threshold values in geochemical data using probability graphs. *J. Geochem.Explor.* 3, (1974),129-149

Satomi, K. and Kruger, P. Radon Emanation Mechanism from Finely Ground Rocks. Stanford Geothermal Program Interdisciplinary Research in Engineering and Earth Sciences. Stanford University, California. (1974).

Tanner, A.B. Radon migration in the ground: a review. In *The natural radiation environment.* Ed. J. Adams and W. Lowder. Univ. Chicago Press, Illinois. (1964). 161-181.

Voltattorni, N. and Lombardi, S. Soil gas geochemistry: significance and application in geological prospectings. In *Natural Gas*. (2010). Ed. P. Potocnik. Sciyo. 183-204.

Voltattorni, N., Sciarra, A., and Quattrocchi, F. The Application of Soil-Gas Technique to Geothermal Exploration: Study of Hidden Potential Geothermal Systems. In *Proceedings*, World Geothermal Congress (2010). 25-29 Apr. 2010. Bali, Indonesia.

Walia, V., Virk, H. S., Yang, F., Mahajan, S., Walia, M., & Bajwa, B. S. Earthquake prediction studies using radon as a precursor in NW Himalayas, India: a case study. *Terrestrial, Atmospheric and Oceanic Sciences* (2005), 16(4), 775-804.